THE COMPRESSION MODES IN NUCLEI - AN EXPERIMENTAL REVIEW

M. Buenerd

JOURNAL DE PHYSIQUE
Colloque C4, supplément au n°3, Tome 45, mars 1984

THE COMPRESSION MODES IN NUCLEI - AN EXPERIMENTAL REVIEW

M. Buenerd

Institut des Sciences Nucléaires, 53, Avenue des Martyrs, 38026 Grenoble Cedex, France

Résumé

La systématique des données sur la résonance monopolaire géante dans les noyaux est présentée et discutée. Les résultats concernant la fréquence du mode monopolaire sont discutés en terme des compressibilités nucléaires pour les noyaux sphériques. Les effets de déformation et les effets isotopiques observés expérimentalement sont aussi discutés. Les résultats expérimentaux récents sur l'existence d'un mode de compression dipolaire isoscalaire sont revus et discutés. Des perspectives pour l'étude de ce mode sont tracées à partir de résultats théoriques.

Abstract

The systematics of data on the giant monopole resonance in nuclei is reviewed. The results on the monopole frequency are discussed in terms of the nuclear compressibilities for spherical nuclei. Deformation effects and isotopic effects on the monopole mode are also reviewed and discussed. The recent experimental evidences for an isoscalar giant dipole resonance are surveyed and discussed. Prospects for experimental studies of this mode are outlined, based on theoretical predictions.

I - Introduction.

The idea of compressionnal modes of nuclear vibrations goes back to the earlier works on the collective model in the years 1960 /1/. However the scientific community had to await some 15 years before the first experimental indication for a nuclear compression mode was reported at Orsay /2/, and two more years before a convincing evidence for a monopole vibration in ^{208}Pb was obtained from small angle measurements at Texas A & M /3/. Since then, extensive studies of this mode and observation of other modes have been reported (see ref.4 for more historical details). In this talk, I shall survey the main experimental results obtained on the giant monopole resonance (GMR) and some more fragmentary indications obtained on the (isoscalar compressionnal) dipole mode (ISGDR). The problem of the higher multipolarity modes will be only briefly discussed to the light of the recent results obtained at Saclay. I shall not discuss the isovector compressionnal modes for, to my knowledge, no experimental results concerning these modes has been reported yet.

Compression modes of nuclei are predicted in many theoretical approaches. The simplest hydrodynamical (liquid-drop) description /5/ of the nuclear motion generates a set of compressionnal eigenmodes, the lowest one being the monopole at 65 $A^{-1/3}$ MeV. Other hydrodynamical approaches of the nuclear collective motion /6,8/ also predict a set of compression modes. However these theories are based on the assumption of local equilibrium in which the motion propagates via two body

collisions, i.e. in which the nucleon mean free path (mfp) is small with respect to the nuclear sizes. This assumption is in severe conflict with the accepted values of the nucleon mfp inside the nucleus, which is of the order of the nuclear radius. Recently, fluid dynamics theories, properly taking into account this basic feature of the nuclear motion, have been developped /7,8,9,10/. They also predict compressionnal high frequency modes varying as $A^{-1/3}$. Although the very nature of giant resonances (zero-sound collisionless modes or first sound modes) is still widely controversial /7,8,9/, all macroscopic theories do predict compression related modes of nuclear vibration.

In the microscopic theories, identifying a compression mode is in principle more delicate. However, comparison of the transition densities predicted by microscopic calculations with those obtained from macroscopic theories allows to identify the compression modes in the set of microscopic states /11,12/. Indeed in macroscopic theories, the compression modes transition densities have one or more node in the surface region. De Haro et al. /11/ use this criterium together with the requirement of a small electromagnetic transition strength to select the compression modes produced in their continuum RPA calculations. Similarly,striking analogies have been noted by B. Bonin /12/ between macroscopic and RPA microscopic /13/ transition densities of states in the same excitation energy range.

This brief overview of the theoretical aspect of the problem, was to show that compression modes appear naturally in any realistic theory of the nuclear motion.

A highly stimulating aspect in the experimental study of the nuclear compression modes lie in their relationship to the nuclear incompressibility K_∞ /10/. The latter is a bulk parameter of nuclear matter (curvature radius of the phase diagramm around the equilibrium), which experimental determination was eagerly waited for by the community of theorists, mainly because of the high sensitivity of this quantity to the microscopic effective interaction used in calculations /14/. Although the relationship between K_∞ and the nuclear compression modulus K_A which is derived from the experimentally measured vibration frequencies suffers some ambiguities /14,15/. The stakes are high enough to provide strong incentives for intensive search and study of these modes.

THE GIANT MONOPOLE RESONANCE

After the first evidences have been obtained for the giant monopole resonance (GMR) in ^{208}Pb /3/ (see other refs in the recent reviews /4,16/ on the subject), study programms have been developped in several laboratoires. Table 1 summarizes these studies. Extensive systematics have been undertaken at Texas A & M on 15 nuclei and at Grenoble on 48 nuclei. Nowaday, the GMR has been unambiguously identified in many nuclei with $A \gtrsim 60$. The situation for light nuclei is more ambiguous as we shall see in the following.

Table 1

Lab.	Projectile	Incident energy (MeV)	Refs.
Grenoble	^3He	108.5	23, 27, 30
Julich	^4He	100 - 172.5	18
Oak-Ridge/Indiana	^4He	152	19
Orsay	d	108	20
Osaka	^3He	120	21
Saclay	^4He	320 - 480	12
Texas A & M	^4He	96 - 129	22, 31

A - Specific experimental aspects of GMR Study.

Before we proceed to the systematics of the results, it is useful to review a few basic physical aspects of the GMR studies with hadron probes having important experimental implications.

An experimental study of the GMR and more generally of any monopole transition with a strongly absorbed projectile like π, d, ^{3}He, ^{4}He and light heavy ions, requires measurements at very small momentum transfer. The reason for that is simple /23/. These reactions are very diffractive and the resulting angular distributions can be approximately described by squared spherical Bessel functions $|J_L(qR)|^2$ with L multipolarity of the transition, q momentum transfer and R strong absorption radius. For monopole transitions the cross-section is maximum at the minimum momentum transfer corresponding to zero degree scattering angle. This already provides a strong motivation to measure inelastic spectra at small scattering angles, but another aspect of the problem makes it simply necessary. Beyond the first minimum of J_0, the monopole and quadrupole angular distributions

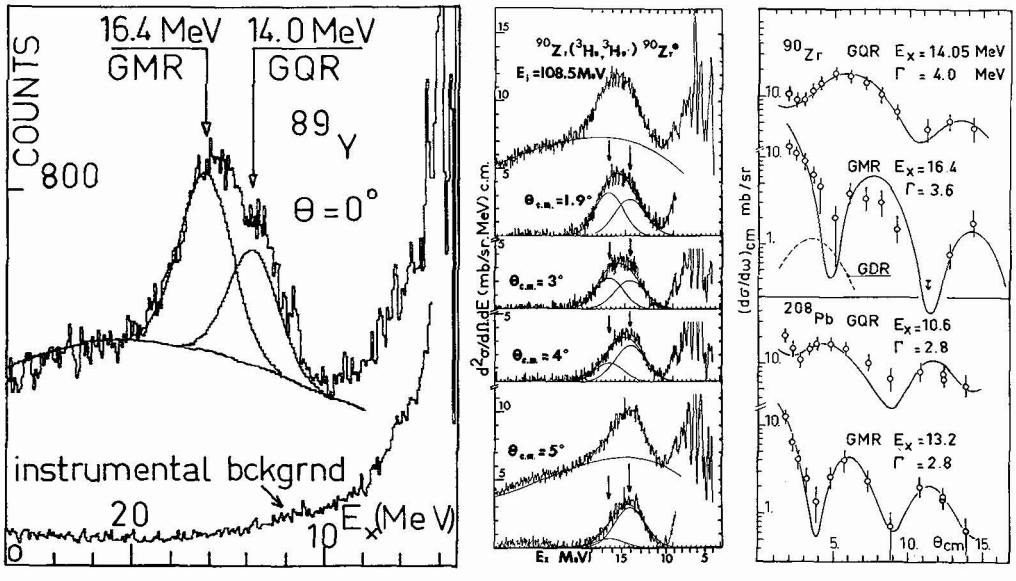

Fig. 1 - Left : inelastic spectrum measured a 0° scattering angle with 108.5 MeV ^{3}He projectile. The unraveling of the spectrum into GMR, GQR and background is shown. Note the large GMR cross-section and the good subsequent accuracy on its excitation energy and strength. Middle : Same reaction on ^{90}Zr at small scattering angles. Note the rapid drop of the GMR cross-section with the increasing angle. Beyond 4° the GMR is completely obscured by the GQR. Right : corresponding angular distributions for ^{90}Zr and ^{208}Pb (see also fig. 2) /22/.

are in phase (Blair rule). This gives rise to ambiguities in multipolarity assignment, which raises a serious problem in the present case because of the proximity of the GMR and the GQR (giant quadrupole resonance), which cross-sections widely overlap in the spectra and are very delicate to disentangle from each other. It is therefore necessary to obtain a set of spectra in which the relative yield of the GMR and GQR are as different as possible, to allow a clean separation of the two components with as less ambiguity as possible. These conditions can be met at the small scattering angles over a range extending from zero degree to around the first minimum of $J_2(qR)$, i.e. covering the region where monopole and quadrupole angular

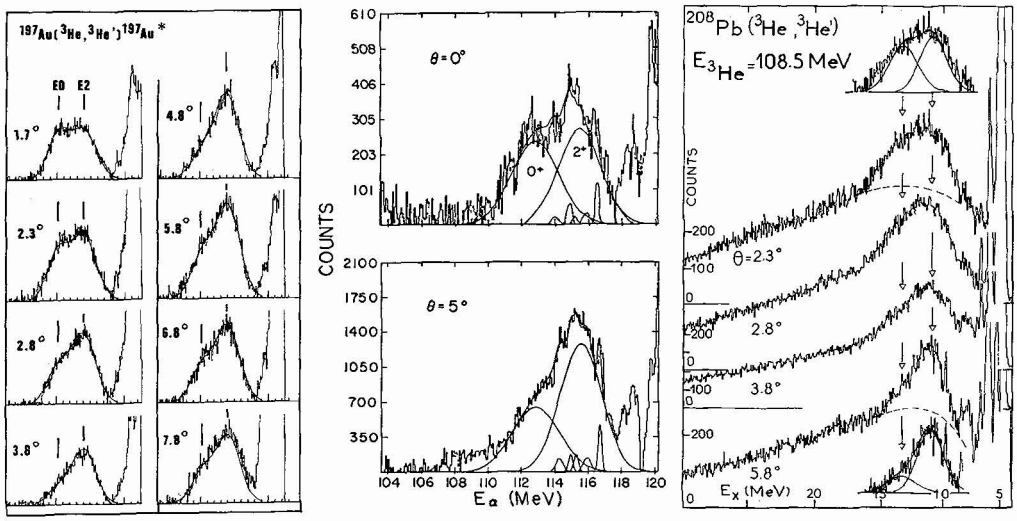

Fig. 2 - Inelastic spectra measured at small scattering angles on heavy nuclei. The GMR and GQR components clearly appear at the smallest angles. Left and right : Grenoble data /4, 17/ ; middle : Texas A & M data on ^{208}Pb /16/. see also ref. 21.

distributions are different /4, 22/. An example is shown on figure 1 to illustrate this problem. The instrumental aspect of small angle measurements has been developped in references 4 and 23.

In the following, the results of DWBA analysis of the data will be presented. In all cases, except specified, they have been performed in the usual framework (see ref. 4 for example) originally defined by R. Satchler /24/.

The (isovector) giant dipole resonance (GDR) is located at the same excitation energy than the GMR and we have shown recently that the cross-section for (coulomb) excitation of the GDR becomes as large as that for the (nuclear) excitation of the GMR at small scattering angles with Helium projectiles of incident energie per nucleon beyond say, 50 to 100 MeV /25/. At most of the energies discussed in the following ($E/A \lesssim 50$ MeV) the GDR cross-section is small enough to be neglected/4,26/.

In the following sections we shall review the available data and concentrate on the systematic small angle measurements performed at Texas A & M and Grenoble.

B - REVIEW OF THE DATA.

B1. HEAVY SPERICAL NUCLEI ($A \gtrsim 140$).

This is the region the mass where the GMR was first observed. For these nuclei the two components, GMR and GQR appear well distinguishable in a clearly double peaked structure in small angle spectra. (figure 2). At the smallest angles investigated the two components clearly show up in the difference spectrum, whereas beyond $\theta \sim 3°$ the monopole peak becomes much smaller and the unraveling of the spectrum is much more uncertain. Figure 2 also compares the results obtained at Texas A & M (ref. 16) and Grenoble on ^{208}Pb. In this region of mass the excitation energy difference between the quadrupole and the monopole mode amounts to around $17A^{-1/3}$ (MeV), i.e. 3 MeV in ^{197}Au, and the widths are about 2.5 - 3 MeV for the two modes. In the region of mass $A \sim 200$, the monopole strength deduced from DWBA analysis approximately depletes the sum rule limit (see table 2). Then , in these nuclei the GMR appears as a very collective state, as are the other giant modes.

B2. MEDIUM MASS NUCLEI ($80 \lesssim A \lesssim 140$).

Figure 3 shows a sample of spectra measured in this region of nuclear masses (see also fig. 1). In these nuclei the two components in the GR peak do not show up as clearly as they do in heavy nuclei, because the excitation energies of the two modes are getting closer to each other with the decreasing mass, and also because the two components are wider (3.5 to 4 MeV) than in heavy nuclei. This makes more difficult to disentangle the monopole from the quadrupole peak in the experimental bump. The existence of the two components is inferred from the shift of the centroïd of the experimental bump observed between say 0° and 5° scattering angles. Indeed, such an effect cannot be accounted for by assuming the excitation of a single nuclear state in the spectra. Beyond $\theta \sim 4°$ the quadrupole peak approximately accounts for the whole bump and the spectra beyond 4° determine the excitation energy E_x and width of the GQR. These values are then used in an iterative procedure to obtain E_x and for the GMR from the spectra with $\theta \lesssim 4°$. Like in heavy nuclei, the unfolding of the two components leads to angular distributions which are in good agreement with DWBA calculations as seen on figure 1. In this region of mass the transition strength is found markedly smaller than in heavy nuclei. It is typically around 40 to 60 % EWSR. This decrease takes place smoothly with the decreasing mass (fig. 5).

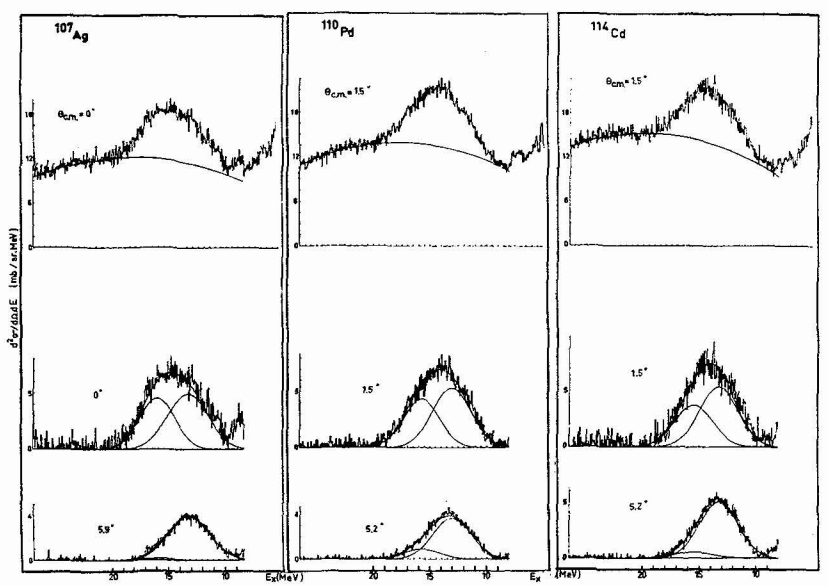

Fig. 3 - small angle inelastic spectra measured with 108.5 MeV ^{3}He on medium mass nuclei. Upper : raw spectra with background shown. Lower : difference spectra at very small angle and around 5°. The GMR is clearly seen at the smallest angle.

B3. LIGHT NUCLEI ($A \lesssim 70$).

The trends observed in heavier nuclei extend down to this region of nuclear mass. In the nuclei ^{64,66,68}Zn (refs.17,28) and ^{58,60}Ni isotopes /27/ it is still possible to distinguish and unfold the two components using the technique explained above. However this becomes increasingly difficult for the excitation energies of the two modes are getting closer (less than one MeV different). The example of the ^{58}Ni is shown on figure 4. Concerning this nucleus and several other light nuclei, we observe that the conclusions reached at Texas A & M and Grenoble are in disagreement

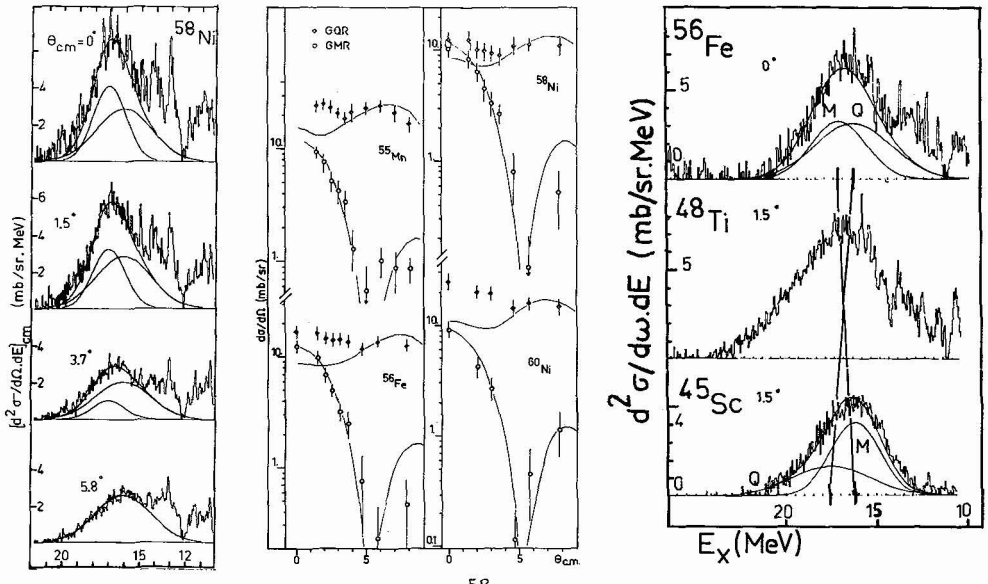

Fig. 4 - Left : difference spectra from ^{58}Ni showing the decomposition of the GR peak into monopole and quadrupole components (higher and lower E_x respectively). Middle : corresponding angular distribution for nuclei of mass A ∿ 60. Right : for A ≳ 50 the monopole strength is found above the GQR. For A ∿ 50 the two components (if two) cannot be unfolded. For A ≲ 50 the monopole strength is found below the GQR. Data from 108.5 MeV ^{3}He scattering/17, 27/.

/22, 27/. In the following of this paragraph I discuss the Grenoble results. A monopole peak is still found in ^{56}Fe and ^{55}Mn nuclei, but when one goes further down in mass (^{51}V, ^{48}Ti) it is no more possible to isolate a monopole peak in the inelastic spectra, for the centroid of the GR peak does not shift with the scattering angle. One has then to rely to the DWBA analysis of the angular distribution of the whole peak to infer the existence of a monopole strength. However such a procedure is much more ambiguous, and no definite conclusion could be reached yet for these nuclei. Nevertheless, in the nucleus ^{45}Sc a monopole peak has been isolated below the quadrupole peak /7/. Since a monopole strength has been found or suggested below the GQR in nuclei ^{40}Ca, ^{27}Al and ^{12}C, one may think that the two modes are really crossing in the region A ∿ 50. Figure 4 (right) shows a comparison supporting this conclusion. The evolution of the relative position of the monopole and quadrupole peaks which is found inverted in ^{56}Fe and ^{45}Sc, suggests that they cross in the region of mass A ∿ 50. Some angular distributions for the GMR and GQR are shown on figure 4.

In this region of mass the strength found in the monopole peak keeps decreasing whith A, the monopole strength is found to deplete only 5 to 10 % EWSR.

More recently, appreciable amounts of monopole strength have been observed in ^{40}Ca (30 % EWSR) and ^{24}Mg (20% EWSR) at Groningen, in ^{24}Mg and ^{28}Si at Heidelberg and in ^{48}Ca (6% EWSR) at Orsay /29/.

B4. SUMMARY OF THE RESULTS.

Figure 5 summarizes the results obtained at Grenoble for the excitation energy, width and reduced transition probabilities of the GMR. The corresponding numbers are given in table 2 along with those from other recent experiments.

The dependence of the excitation energy on the nuclear mass is found different from the empirical law $80A^{-1/3}$ MeV (dashed line) suggested from previous works. The solid line on figure 5 corresponds to a best fit obtained with a hydrodynamical formula. It will be discussed in details further below. The bending down of E_x (GMR) with the decreasing mass is understood as a surface compressibility effect.

The width (FWHM) of GMR (figure 5 - 6) increases with the decreasing mass between A $\sim$ 232 and A $\sim$ 90 as it does for the other known giant modes. However below A $\sim$ 90, it is found to decrease. The behaviour of the width in the region A $\sim$ 90 is reasonably accounted for by a viscous hydrodynamical model /6/, but the disagreement is sharp for A < 90. Note however the different values obtained for the GMR width in Zn isotopes at Texas A & M /16/.

As we have already pointed out, the reduced transition probability deduced from DWBA analysis is observed decreasing from around 100 % EWSR in heavy nuclei (A $\sim$ 100), down to 10 % EWSR in light nuclei (A $\sim$ 27-60). Figure 5c shows that this dependence is roughly linear through the mass table for spherical nuclei (dashed line). This result is not understood at present and requires a theoretical interpretation. For example RPA calculations predict in ^{40}Ca a GMR depleting 88 % EWSR /14/, whereas an upper limit based on the experimental data /27/ was set at 12.5 % EWSR. A single peak exhausting 88 % EWSR would correspond to around 80 mb/sr, representing 5 times the total cross - section (GQR + GMR) found section at the smallest angles is between 10 mb/sr in light nuclei and 30 mb/sr in heavy nuclei, i.e. different by a factor of 3 whereas the corresponding sum rule fractions differ by a factor of 10 to 20. This questions the goodness of the transition density based on the scaling approximation and used in the DWBA analysis. Indeed, it has been suggested recently that this transition density might miss another surface contribution /14/. This point should be investigated. The folding model analysis of G.R. Satchler /19/ generally leads to larger reduced transition probabilities both in light and heavy nuclei. Note also the possibility of another mode at higher E_x /50/.

Another interesting feature of the systematics of the GMR strength lies in the two dips oberved on fig. 5 in the regions of mass 140 $\lesssim$ 200 and 90 $\lesssim$ A $\lesssim$ 110. We are going to see in the next section that these dips, which extend over two regions of nuclear deformation, can indeed be attributed to a deformation effect on the GMR.

B5. DEFORMED NUCLEI.

Figure 6 displays partial systematics of E_x (GMR) as a function of the mass number. In the regions of deformed nuclei, 144 $\lesssim$ A $\lesssim$ 197 and $\sim$ 230, the values of E_x are enhanced compared to those of the nearby spherical nuclei A $\sim$ 140 and A $\sim$ 200 making a broad bump on the average shape of the systematics. Figure 6 shows the difference ΔE_x between the experimental values E_x and the values E_{hyd} obtained with the hydrodynamical formula (3) after a fit of its parameters to the data on spherical nuclei (ref. 30). The same conclusion is reached by simply interpolating between the values in the spherical regions A $\sim$ 140 and A $\sim$ 200. Figure 6b also shows the experimental deformation parameters β for the ground state of the studied nuclei.

The correlation ΔE_x and β appears clearly for all but one (^{152}Sm) nuclei. Assuming a linear dependence between ΔE_x and β leads to $\Delta E_x/\beta = 1.8 \pm 0.9$ MeV. Figure 6c shows the same GMR strength than fig. 5c. The slightly different numerical values compared to ref. 3 due to the use of different optical parameters in the DWBA analysis. The depletion observed in the deformed region suggests that the missing strength might be carried out by a splitted component.

A comparative study of the spherical ^{144}Sm and deformed ^{154}Sm nuclei has lead the Texas A & M group to the conclusion that the monopole strength is splitted in deformed nuclei /31/. This is seen on fig. 7 (upper) where the small angle spectra

Table 2 - GQR and GMR excitation energy E_x, width (FWHM)Γ and strength S, measured at Grenoble (GR, refs. 23,27,30), Julich (JUL,ref 18),Oak-Ridge/indiana (OA, ref19), Orsay (ORS, ref20), and Texas A & M,(TAM refs22,31). See also ref. 21 and communications to this conference.

Nucleus	GMR E_x MeV	GMR Γ MeV	GMR S % EWSR	GQR E_x MeV	GQR Γ MeV	GQR S % EWSR	Ref
^{27}Al	17.15±0.2	2.5 ±0.4	6	19.3 ±0.5	6.5 ±0.5	44	GR
	not observed			20.1 ±0.3	7.6		TAM
^{40}Ca	(16-18)		(8)	18.2 ±0.3	3 ±0.3	34	GR
	not observed			17.7 ±0.3	2.5		TAM
^{45}Sc	16.1 ±0.5	3.25±0.7	10	17.6 ±0.7	5.3 ±0.7	33	GR
^{46}Ti	not observed			17.6		50	OA
^{48}Ti	not observed			17.1 ±0.4	(5.3)		GR
				16.2 ±0.4	4.5 ±0.5		TAM
^{51}V	not observed			17.2 ±0.4	5. ±0.4		GR
^{55}Mn	17.7 ±0.5	4 ±0.5	10	16.25±0.5	6 ±0.5	55	GR
^{56}Fe	17. ±0.3	3.6 ±0.3	10	16.2 ±0.3	5 ±0.4	44	GR
^{58}Ni	17.1 ±0.3	2.5 ±0.3	10	16.2 ±0.3	4.25±0.4	43	GR
	not observed			16.4 ±0.2	4.9 ±0.2		TAM
	20		40	16		45	OA
^{60}Ni	17 ±0.3	2.7 ±0.3	8	15.9 ±0.3	5 ±0.4	53	GR
^{64}Zn	18.2 ±0.5	4.3 ±0.9	29±16	15.3 ±0.3	4.7 ±0.4	38±10	TAM
^{66}Zn	17.9 ±0.25	2.4 ±0.25	16	14.8 ±0.25	4 ±0.2	80	GR
	18.4 ±0.7	4.1 ±1.1	30±16	14.9 ±0.5	4.5 ±0.5	38+10	TAM
^{68}Zn	17.8 ±0.25	3 ±0.3	18	14.6 ±0.2	4 ±0.2	90	GR
^{89}Y	16.35±0.25	3.1 ±0.25	47	13.85±0.25	3 ±0.25	39	GR
^{90}Zr	16.4 ±0.25	3.6 ±0.25	39	14.05±0.25	4 ±0.25	49	GR
	16.2 ±0.5	3.5 ±0.3	90±20	14 ±0.2	3.4 ±0.2	66±17	TAM
	17		80±20	14.1		65	OA
	17.2 ±0.5	4.3 ±0.3	25±8	14.1 ±0.5	4.3 ±0.3	50±10	ORS
^{96}Zr	15.8 ±0.3	3.2 ±0.3	28	13.3 ±0.3	3.8 ±0.3	45	GR
^{92}Mo	16.35±0.3	4 ±0.3	24	14.55±0.3	4.25±0.3	44	GR
^{96}Mo	16.4 ±0.3	3.5 ±0.3	19	13.75±0.3	4.25±0.3	50	GR
^{100}Mo	16 ±0.45	3.75±0.45	17	13.3 ±0.3	4.6 ±4.5	76	GR
^{107}Ag	15.9 ±0.3	3.7 ±0.35	26	13.35±0.3	4.2 ±0.35	53	GR
^{108}Pd	16.25±0.3	4 ±0.3	29	13.25±0.25	3.9 ±0.3	65	GR
^{110}Pd	15.7 ±0.3	3.75±0.35	42	13 ±0.3	4 ±0.4	53	GR
^{110}Cd	15.95±0.25	4.15±0.25	36	13.3 ±0.25	4 ±0.25	60	GR
^{112}Cd	15.75±0.25	3.6 ±0.35	43	13.5 ±0.25	4 ±0.35	74	GR
^{114}Cd	15.45±0.25	4 ±0.4	53	13.25±0.25	4 ±0.4	74	GR
^{116}Cd	15.75±0.25	3.4 ±0.30	53	12.95±0.25	4 ±0.3	88	GR
^{115}In	15.9 ±0.3	2.7 ±0.3	27	13.3 ±0.3	3.3 ±0.3	100	GR

Nucleus	GMR E_x MeV	GMR Γ MeV	GMR S % EWSR	GQR E_x MeV	GQR Γ MeV	GQR S % EWSR	Ref
^{112}Sn	16.1 ±0.25	3 ±0.25	42	13.65±0.2	3.6 ±0.2	55	GR
^{116}Sn	15.55±0.25	3.2 ±0.3	45	13.15±0.25	3.6 ±0.3	60	GR
	15.6 ±0.3	4.1 ±0.3	180±60	13.2 ±0.2	3.3 ±0.2	84±25	TAM
^{118}Sn	15.5 ±0.6	4.1 ±0.7	≥150	13.2 ±0.3	3.5 ±0.3	≥60	TAM
^{120}Sn	15.45±0.25	3.25±0.3	50	12.75±0.25	3.75±0.3	82	GR
	15.2 ±0.5	4.1 ±0.6	≥180	12.7 ±0.4	3.5 ±0.4	≥80	TAM
	16.9		100±20	13.3		70±15	OA
	16.1 ±0.4	4 ±0.4	64±15	13.2 ±0.2	4 ±0.3	69±10	ORS
^{124}Sn	14.85±0.25	3.2 ±0.3	58	12.35±0.25	3.6 ±0.3	88	GR
	14.8 ±0.4	3.8 ±0.6	186±60	12.3 ±0.4	3.1 ±0.3	78±25	TAM
^{139}La	15. ±0.25	2.7 ±0.25	59	12.25±0.25	3.1 ±0.3	68	GR
^{140}Ce	14.8 ±0.2	3.0 ±0.2	57	12 ±0.15	3 ±0.2	79	GR
^{141}Pr	14.9 ±0.25	2.6 ±0.25	63	12.2 ±0.25	3 ±0.3	66	GR
^{144}Sm	14.7 ±0.2	2.9 ±0.2	64	12.25±0.2	2.5 ±0.2	50	GR
	14.6 ±0.2	3 ±0.3	140±40	12.2 ±0.2	2.4 ±0.2	45±15	TAM
	15.5 ±0.5	2.9 ±0.5	100±20	12.8	2.8 ±0.3	80	OA
^{150}Sm	15.1 ±0.25	3 ±0.25	49	12.3 ±0.2	3 ±0.2	76	GR
^{152}Sm	14.8 ±0.25	3.1 ±0.25	42	11.95±0.2	3 ±0.2	81	GR
^{154}Sm	15 ±0.3	3.3 ±0.3	44	11.7 ±0.25	3.75±0.25	81	GR
	14.9 ±0.3	2.6 ±0.4	55±15	11.8 ±0.3	3.7 ±0.3	55	TAM
	15.5						OA
^{159}Tb	14.85±0.25	3.4 ±0.25	42	11.75±0.25	3.6 ±0.25	70	GR
^{165}Ho	15. ±0.25	2.7 ±0.3	41	11.9 ±0.35	3.8 ±0.3	77	GR
^{169}Tm	14.7 ±0.3	2.5 ±0.3	40	11.6 ±0.25	3.15±0.25	86	GR
^{175}Lu	14.4 ±0.3	3 ±0.3	55	11.6 ±0.3	2.75±0.3	76	GR
^{181}Ta	14.2 ±0.25	2.5 ±0.25	59	11.3 ±0.25	3.25±0.25	78	GR
^{197}Au	13.45±0.2	2.4 ±0.2	99	10.95±0.2	2.6 ±0.2	100	GR
^{208}Pb	13.2 ±0.3	2.8 ±0.25	92	10.6 ±0.25	2.8 ±0.25	100	GR
	13.7 ±0.4	3 ±0.5	90±20	11 ±0.2	2.7 ±0.3	105±25	TAM
	13.8 ±0.3	2.6 ±0.3	85	10.9 ±0.3	2.6 ±0.3	70	JUL
	13.9		100±20	10.9		77±15	OA
	13.5 ±0.3	2.8 ±0.2	51±10	10.5 ±0.2	2.8 ±0.2	104±15	ORS
^{209}Bi	13.3 ±0.3	2.3 ±0.3	108	10.7 ±0.3	2.8 ±0.3	120	GR
^{232}Th	13.35±0.4	2.3 ±0.4	84	10.9 ±0.4	2.7 ±0.4	81	GR
	13.8 ±0.4	3 ±0.5	66±13	10.9 ±0.3	3 ±0.4	62±12	JUL
	9.6 ±0.3	2.3 ±0.3	28 ±6				
^{238}U	13.7 ±0.4	3 ±0.5	65 ±13	10.8 ±0.3	3 ±0.4	66±13	JUL
	9.3 ±0.3	2 ±0.3	30 ±6				

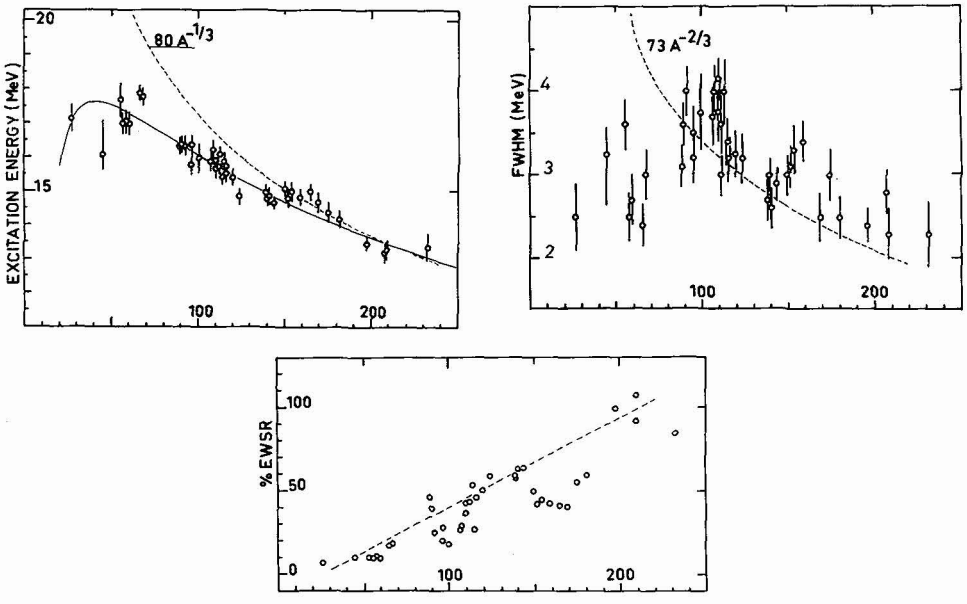

Fig. 5 - Systematics of (a) excitation energy, (b) width (FWHM), and (c) reduced transition probability (% EWSR) of the giant monopole resonance, as obtained from inelastic scattering of 108.5 MeV ^{3}He at Grenoble /17/. The numerical values are given in table 2.

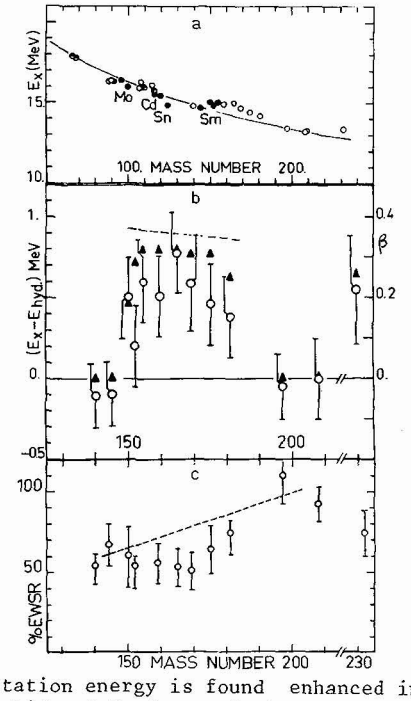

Fig. 6 - (a) the GMR excitation energy is found enhanced in the actinides region. (b) the upwards shift of E_x (open circles, scale at left) is found correlated with the ground state deformation (triangles, scale at right). (c) the monopole transition strength is found depleted in deformed nuclei (see also fig.5).

clearly show that the cross-section for the upper peak is smaller in ^{154}Sm than in ^{144}Sm whereas the opposite is true for the cross-section of the lower peak, the total cross-section being the same in the two nuclei. This is interpreted by assuming that in the deformed ^{154}Sm, the GMR is splitted into two components, the lower one being mixed with the GQR. The same reults have been obtained later at Grenoble as shown on lower fig. 7.

More recently the study of the two actinide nuclei ^{232}Th and ^{238}U has been performed at Julich using (α,α') reaction at two incident energies (second ref.18). From the comparison of the two sets of data, the authors have isolated the cross-section of the lower component of the GMR (see table 2).

The experimental results are rather well explained in terms of a coupling of the GMR and the GQR due to the static deformation of the nucleus /4, 30, 32/. Abgrall et al. /32/ predict that the GMR main component should shift to higher excitation energy by $\Delta E_x \sim 5A^{-1/3}$ MeV for a deformation $\beta = 0.3$, in reasonable agreement with the experimental results (dashed line on fig. 6).

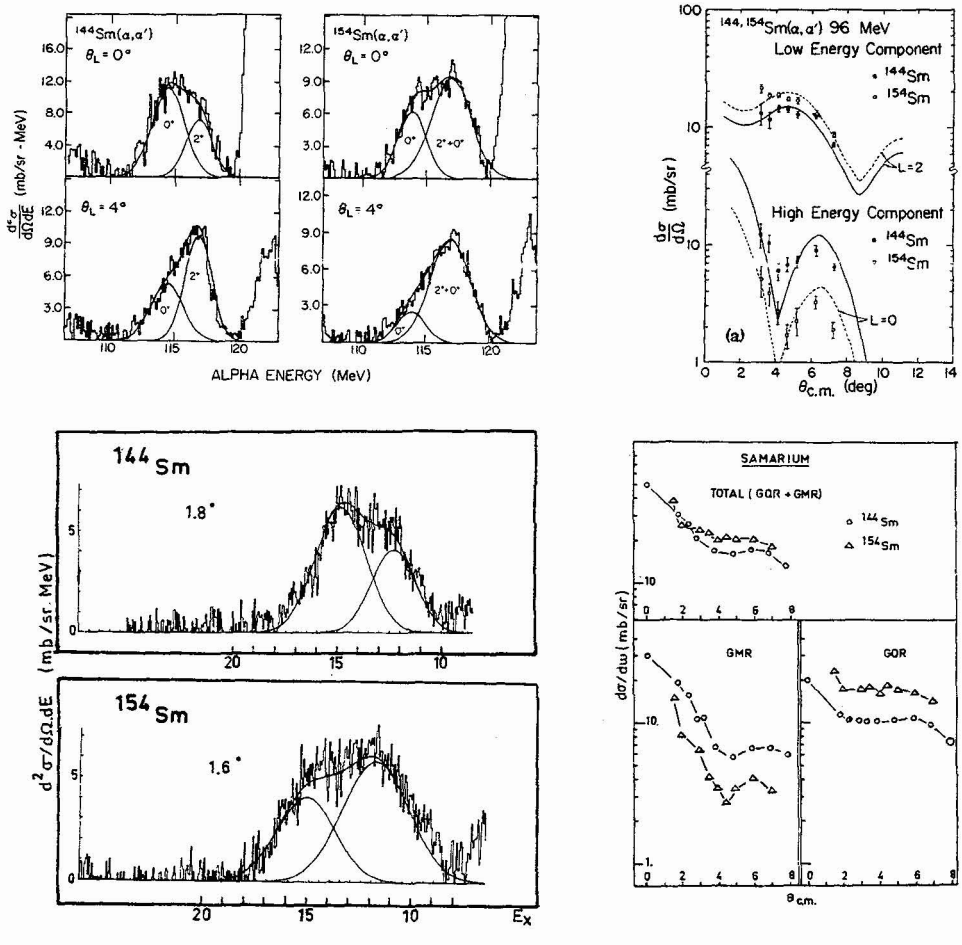

Fig. 7 - inelastic data in the GR region for spherical ^{144}Sm and deformed ^{154}Sm measured at Texas A & M /31/ (upper) and Grenoble /17/ (lower).

We have already mentionned the existence of a second dip in the region A ∿ 90 - 110 of the systematics of the GMR strength (fig. 5). It is tempting to infer from this observation that it could have the same origin (deformation) as the one observed in the rare earths and actinides discussed above. We believe this hypothesis to be basically correct although the shift on the excitation energy of the main (upper) GMR component is mixed with another (isotopic) effect (see below). Two arguments are strongly supporting this conclusion. First, this region of mass is known to exhibit appreciable ground state deformation /30/, and the deformation effect observed in heavy deformed nuclei is bound to manifest itself also in these nuclei. Further, a deformation effect has been observed previously on the GDR of the Molybdenum isotopes in γ absorption experiments /34/. In these experiments the spreading of the dipole strength has been found to increase with the increasing mass of the isotope between A = 92 and A ≈ 100, and the width was found to be correlated to the ground state deformation. In the same isotopes the ratio of the GMR cross-section to the GQR cross-section in the zero degree spectra is found to be 1.1, 0·46, 0.32 for ^{92}Mo (β = 0.11) ^{96}Mo (β = 0.17) and ^{100}Mo (β = 0.25) respectively. The firmly supports the existence in this region of nuclear mass of the same deformation effect and then the same coupling between the GMR and the GQR, as observed in heavy deformed nuclei. Figure 8 displays the ratio σ(GMR)/ σ(GQR) at Θ = 0° as a function of the deformation /33/ for a set of nuclei in this region. Most of the values fall approximately along a line. The large sensitivity of this ratio to the nuclear deformation could make it a further mean of investigating small deformation in nuclei.

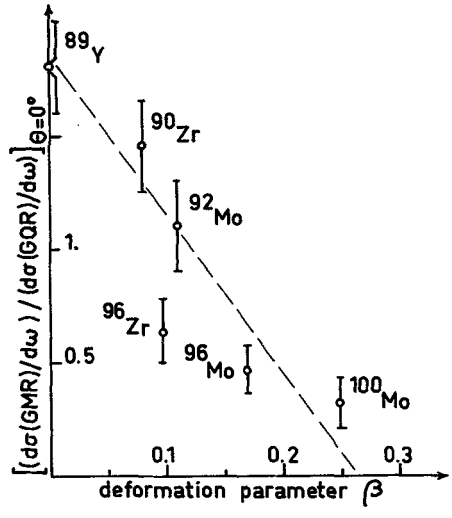

Fig. 8 - Ratio of the GMR to the GQR differential cross-section at zero degree scattering angle plotted as a function of the deformation parameter. For ^{89}Y we have set β ∿ 0 on the basis of the well known quasi-sphericity of the neighbouring nuclei (^{88}Sr, ^{90}Zr). The dashed line is an eye guide.

C - THE NUCLEAR COMPRESSIBILITES.

C1. FRAMEWORK OF THE ANALYSIS.

The theoretical aspects involved in the compressional monopole vibration phenomenon have been extensively investigated in refs. 14, 15. They will not be discussed here. However, in order to give a frame to the following discussion, I have to define the quantities of interest and to come back to some elementary concepts relevant to the field.

The definition of the compression modulus of a nucleus appears naturally when writing the potential energy of the system undergoing a radial isotopic oscillation. Using the root mean square radius r_o as a collective variable, the potential energy of the system in harmonic approximation is given by /35, 36/ :

$$V(r) = V(r_o) + \frac{1}{2} r_o^2 \frac{d^2\varepsilon}{dr^2} \frac{(r-r_o)^2}{r_o^2} + 0$$

$V(r_o)$ being the ground state potential energy and ε the total binding energy of the nucleus. The compression modulus of the nucleus is then defined as :

$$K_A = r_o^2 \frac{d2}{dr^2} \left(\frac{\varepsilon}{A}\right) \tag{1}$$

the macroscopic model of Werntz and Uberall /35/ as well as the microscopic sum rule approach /14/ lead to the following relationship between K_A and the monopole frequency :

$$\hbar\omega = \hbar \left[\frac{K_A}{m\langle r_o^2 \rangle} \right]^{1/2} \tag{2}$$

where m is the nucleon mass. It is interesting to note that the macroscopic model gives rise to the same transition density /36/ as that used as a collective form factor in DWBA calculations, thereby making the analysis completely consistent.

Now one can make a further step by noting that /A can be obtained from the semi-empirical mass formula /19/. This leads to the following expression for the

$$K_A = k_V + k_S A^{-1/3} + k_\tau \left(\frac{N-Z}{A}\right)^2 + k_C Z^2 A^{-4/3} \tag{3}$$

In this relation the ki's are the second derivatives of the corresponding coefficients of the mass formula with respect to r_o. k_C can be obtained analytically /37/

$k_c = \frac{6e^2}{5r}$ (r_c = charge radius).

Empirical values of the k_i parameters can be obtained by putting relation (3) into relation (2) and adjusting the k_i's so as to reproduce the set of experimental values of E_c (GMR).

However, it has been shown by J.P. Blaizot /14/, that relation (3) ignores the equilibrium conditions of the nuclear ground state. A proper treatment of the problem leads to somewhat different and more complicated relation :

$$K_A = K_\infty + [K_{surf} + 4a_{surf}\ (1 + \frac{27}{2} R)]\ A^{-1/3}$$

$$+[K_{sym} + 3L - 27L\ R)]\delta^2$$

$$+ \frac{3}{5}\frac{e^2}{R_o}(1 - 27\ R)\ Z^2\ A^{-4/3} \qquad (4)$$

where notations are the same as in ref./14/ with $R = \frac{n_\infty^2}{K_\infty}\frac{d^3\varepsilon}{dn^3}$

We see by comparing this formula to relation (3), that the general form of the parametrization is the same, only the interpretation of the $A^{-1/3}$ and δ^2 coefficients is changed. Relation (4) can then be rewritten as :

$$K_A = K_\infty + K_\Sigma A^{-1/3} + K_\tau \delta^2 + K_c Z^2 A^{-4/3} \qquad (5)$$

The difference between relations (3) and (5) lies in the value of the coulomb term. For example, using R = 0.25 as justified further below, leads to - 23 MeV for the coulomb contribution in relation (4) instead of 6.55 MeV in relation (3) for the nucleus ^{208}Pb. These different values of the coulomb term directly affect the numerical values obtained for the ki(Ki) fitted to the data /4/.

In relation (4) the quantity a_{surf} is well known empirically, whereas L which is related to the first derivative of the asymmetry energy relative to the density, is not so well determined. Moreover, the theoretical value of the latter critically depends on the effective interaction used. As for the quantity R, working it out from the numbers given in ref. 14 for the various interactions used, leads to a set of values ranging from 0.2 to 0.35. Beside this, the Orsay group has shown, recently /38/ that this quantity can be related empirically to the compression modulus of nuclear matter at saturation density by the relation :

$$n_\infty^2\ (d^3\varepsilon/dn^3) = (\frac{1}{2}K_\infty - 45)\ \ MeV \qquad (6)$$

which can be inserted into relation (4), making then all the term depending on K_∞.

RESULTS.

The various relations given above have been used to analyse the sets of experimental data available. The ki (Ki) parameters have been adjusted using a chi-squared minimization procedure so as to reproduce the experimental monopole frequencies by means of relation (2), K_A being defined according to relation (3) or (5) or (4) + (6). The approach using relation (3) has been used by the Texas A & M group /22/, and the Grenoble group /4, 17, 27/. However we have seen that this approach is questionnable and that the use of relations (5) or (4) + (6) corresponds to a more rigorous treatment of the problem. The results of the analysis are given in table 3. These results have been extensively discussed in ref. 4, then I shall limit myself to a few remarks on the values obtained for the parameters of the compression modulus K_A.

* Volume (K_∞) and surface (K_Σ) terms.

The data on heavy nuclei are not sensitive to the admixture of the (surface) $A^{-1/3}$ term. However, this term is pinned down with a good accuracy by the experimental frequencies in light nuclei (A < 60). This can be seen on fig. 5A where the surface term takes over the volume term in light nuclei (bending down of the curve). However the GMR in this range of nuclear mass depletes a smaller

Table 3 - Compression moduli obtained from the analysis of the GMR data.

Laboratory	K_∞ Volume	K_Σ Surface	K_τ Asymmetry	Number of nuclei fitted	refs.
Grenoble	261.5±7	-542±26	-420±93	33	a,b)
	278±8	-591±20	-432±85	33	a,c)
	268±4	-579±15	-296±94	33	(4) b,d)
Orsay analysis, data from					
Texas	357±35	-883±148	-492±210	9	
Grenoble	300±29	-608±120	-475±176	18	(40)
Average	220±20	-240±70	-300		e)

a) fit performed with $\langle r^2 \rangle = 3/5(1.12\ A^{1/3})^2\ (1 + 3.84\ A^{-2/3})$; b) use of relation (5) ; c) use of relations (4) + (6) ; d) use of $\langle r^2 \rangle$ from ref. 39 ; e) with $K_\tau = -300$ fixed and $K_\Sigma = -K_\infty$

fraction of the sum rule (figure 5a). This makes the numbers in table 3 somewhat ambiguous. The experimental fact that the missing strength in light nuclei can only be at excitation energies $E_x \gtrsim 30$ MeV implies that the average monopole frequency can only be larger than the values given in table 3, and then that these latter values are upper limits of $|K_\infty|$ and $|K_\Sigma|$

The values of K_Σ in table 3 are somewhat larger than the simple estimate of Blaizot and Grammaticos $K_\Sigma = -440$ MeV. The smaller value used by the Orsay theorist group ($K_\Sigma = 240$ MeV, bottom line in table 3) was dictated by theoretical considerations /40/.

* Isotopic effect and the asymmetry term (K_τ).

The upper figure 9 shows a partial systematics of the GMR excitation energy measured at Grenoble over the mass range $90 < A < 140$. The values of E_x(GMR) for a given element are lying approximately along lines with a roughly constant negative slope, each line making an angle with the overall systematic dependence on A illustrated by the dotted line. Fig. 9 (lower) shows the same GMR excitation energy plotted versus the squared nuclear asymmetry for the studied Zr, Mo, Pd, Cd and Sn isotopes. It shows the same consistent trend of decreasing E_x with the increasing asymmetry, with a roughly constant average slope. A few nuclei such as ^{92}Mo and ^{116}Cd do not follow the general trend. We have seen above that the data in the region of mass $A \sim 100$ exhibit deformation effects which may explain, at least partly these discrepancies. For the Sn isotopes known as sperical, the data points are nicely lined up. Constraining K_τ in relation (5) so as to reproduce this slope leads to $K_\tau \sim -700$ MeV and $K_\infty = 280$ MeV, $K_{surf} = -614$ MeV. However the corresponding value of χ^2 is somewhat larger than the best fit value obtained from the overall fit of the data /4/. Nevertheless this value of K_τ is in quite reasonable agreement with the estimate of Blaizot and Grammaticos /42/ who found $K_\tau \sim -660$ MeV.

On this point, one must note that a similar isotopic effect has been reported concerning also the GQR /41/ and the GDR /34, 43/, which seriously questions its origin. Figure 10 shows small angle spectra from Sn isotopes where one can see that both the excitation energies of the GQR and the GMR shift by about 1.3 MeV between ^{112}Sn and ^{124}Sn.

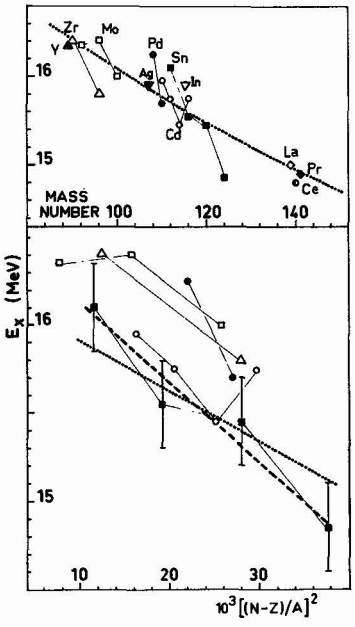

Fig. 9 : Upper : E_x (GMR) as a function of the nuclear mass in the range A ∿ 90 - 140. The dotted line shows the best fit obtained with relation (4) for nuclei along the stability line. Lower : Same as above versus the squared nuclear asymmetry. The dotted line is again the prediction of relation (4) (see table 3, first row) for the Sn isotopes. The dashed line corresponds to K_{sym} = - 700 MeV (see text) for the same isotopes (for details see refs. 4, 41).

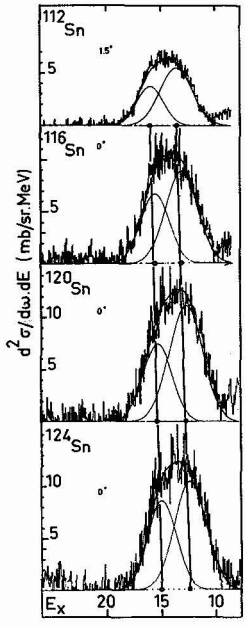

Fig. 10 - Difference spectra of Sn isotopes showing evidence for the isotopic effect affecting both the GMR and the GQR. The lines connect the abcissa of the peak centroïds. The total excitation energy shift between ^{112}Sn and ^{124}Sn amounts to around 1.3 MeV for the two resonances.

THE ISOSCALAR GIANT DIPOLE RESONANCE

In the liquid drop model the first sound dipole mode is predicted at a systematic excitation energy of 93 $A^{-1/3}$ MeV /5/. the other fluid dynamical theories also predict a dipole mode over a range extending from 85 $A^{-1/3}$ /9/ up to about 200 $A^{-1/3}$ /8/ (note however in this latter case, that the high value is due to the large incompressibility produced by the interaction used), whereas in the elasticity approach, the state is found at 77 $A^{-1/3}$ (somewhat below the monopole mode)/10/. The more sophisticated microscopic calculations provide nicely converging results /11, 44, 45/, they all set the isoscalar giant dipole mode between 125 $A^{-1/3}$ and 170 $A^{-1/3}$ MeV in heavy nuclei.

The first experimental indication for a giant isoscalar dipole mode has been obtained from inelastic ^{4}He scattering spectra at 172.5 MeV /46/. In this work the authors have extracted from their data the cross-section of a wide (Γ = 5.9 MeV) peak, centered at 21.3 MeV excitation energy, which angular distribution could be reproduced by DWBA calculations only assuming a dipole transition depleting 90 % EWSR (fig. 11). It has been shown later that this assignment was more ambiguous than first claimed /47/. The analysis of a set of new measurements of the same reaction, extending the data at small scattering angles down to 2.5°, seems to confirm the first assignment (second ref. 47), although the cross-section for the 21.3 MeV peak at angles smaller than $\Theta \sim 5°$, where the comparison with the calculations is most interesting, would make the conclusion even more convincing.

Another experimental result supporting the existence of a giant dipole state around 21.5 MeV in ^{208}Pb has been obtained at Orsay from proton inelastic scattering data at 201 MeV /48/. The spectrum on figure 12 provides a convincing evidence that a wide (Γ = 5.7 MeV) state is excited at 21.5 MeV excitation energy. The excitation energy and width are in good agreement with the ^{4}He scattering results. However, the DWBA analysis of the data shows that they cannot be accounted for assuming a pure $(J^{\Pi},T) = (1^-, 0)$ transition. Electron scattering experiments on the same nucleus have shown the existence of an isovector giant quadrupole state having approximately the same width and excitation energy as the observed peak (see refs. in ref.48). The (p,p') data can be well accounted for by assuming that both $(2^+, 1)$ and $(1^-, 0)$ states are excited in the reaction /48/. This is shown on figure 12. A microscopic DWBA analysis of the same data in second ref. 47 leads to the same conclusion.

A third experimental result has been obtained by the Julich group from fission decay measurements in coincidence with inelastically scattered 172.5 MeV ^{4}He an ^{208}Pb /49/. In this work the 20 MeV excitation energy region was found to have a surprisingly large decay probability to the fission channel and the measured angular correlation is in agreement with the L = 1 and 3 multipolarity assigned in this region of excitation energy.

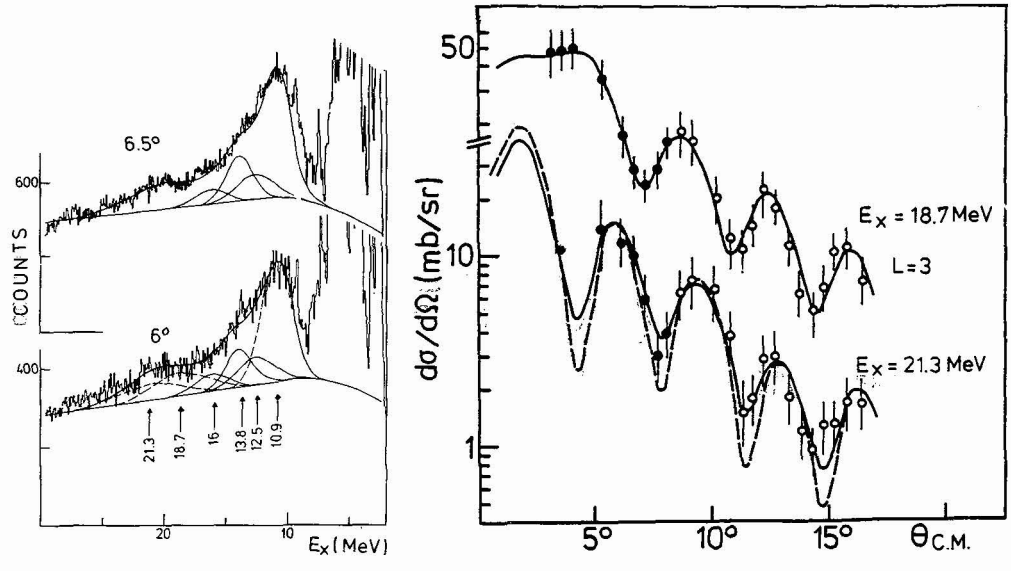

Fig. 11 - left : inelastic ^{4}He spectra showing excitation of a broad structure around 20 MeV in ^{208}Pb. Right : angular distributions of the octupole and dipole component unfolded from the data /46/.

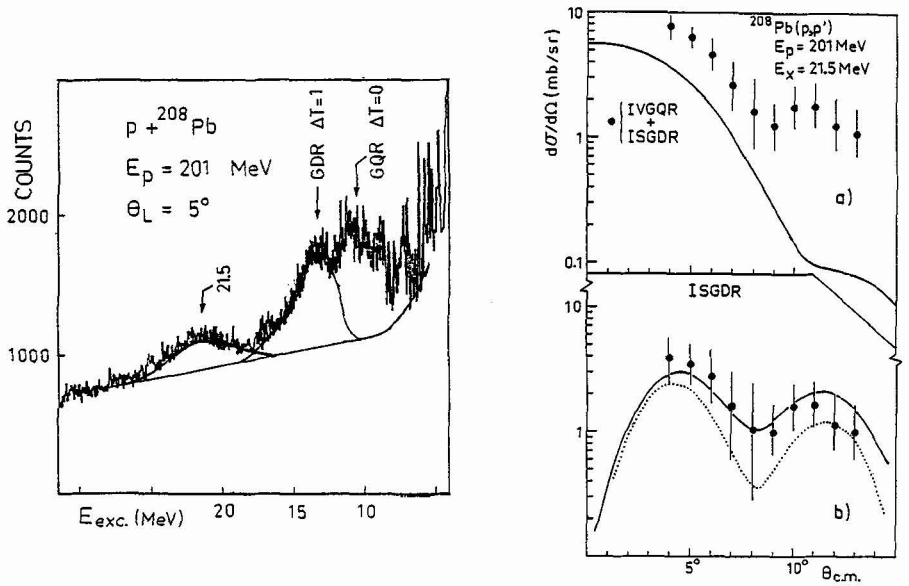

Fig. 12 - left : inelastic proton spectrum showing the excitation of a broad peak at 21.5 MeV in ^{208}Pb. Right : experimental angular distribution of the peak and theoretical value for coulomb excitation of the isovector GQR (upper). The difference (lower) is accounted for by a calculations assuming an isoscalar dipole transition /48/.

The above results are not in very good agreement with those obtained recently at Saclay from 340 and 480 MeV ^{4}He scattering study, for the excitation energies, although the strengths found are comparable /12/ (figure 13). Positive indication for the GDR is also available from inelastic (π,π') data /52/.

From this set of experimental results, we can conclude to a reasonable evidence for an isoscalar GDR in ^{208}Pb. However this result should be confirmed with other probes and a search for the ISGDR should be conducted in other nuclei before a definitive conclusion can be drawn.

Concerning the point of looking for such a state in other nuclei, it is interesting to underline the goog agreement with the experimental results mentionned above and the continuum RPA calculations. In ref. 11 as well as in ref. 44, the isoscalar dipole strength in ^{208}Pb is found concentrated in a peak centered at 22 MeV, with a width of about 4 - 5 MeV and exhausting 60 % of the sum rule. These numbers are remarkably close to the experimental values. This agreement gives confidence in the calculations on other nuclei (note however that the agreement is less good for the GMR /44/). In ^{90}Zr, Van Giai and Sagawa predict 73 % EWSR in a 7 MeV wide peak centered around E_x = 30 MeV /44/. Such a strength should probably be observed in the same conditions as for ^{208}Pb. In ^{40}Ca, the strength is probably too much widespread ($\sim$ 20 MeV) to be observed experimentally. Finally I would like to emphasize that a systematic experimental search for the $(1^-, 0)$ strength in nuclei with $90 \lesssim A \lesssim 200$ is of major importance to establish a definitive status for the isoscalar dipole compressional mode of nuclear vibrations.

HIGHER MULTIPOLARITY COMPRESSIONNAL MODES

To finish this talk I would like to outline a few prospects concerning the higher compressionnal modes. I believe the results summarized on figure 13 provide an interesting ground for such a discussion /12/.

Let us note first some features of the theoretical approaches relevant to this point. A common prediction of both macroscopic /8, 12, 50/ and microscopic /11/ theories concerns the second monopole $(0_2^+,0)$ compressionnal mode consistently located in the 25 - 35 MeV excitation energy region of ^{208}Pb carrying a small fraction of the EWSR /11/. No experimental indication has been reported yet supporting the existence of such a transition strength. For the quadrupole mode, the location of the strength vary by a factor of about 4 depending on the theoretical approach. The RPA results /11/ locate it around E_x = 30MeV (10%EWSR).For the higher multipolarities the dispersion of the theoretical predictions becomes even worse. One must note the large spreading of the $(3^-,0)$ and higher L compressionnal strength obtained in continuum RPA calculations /11/ which leave little hope that these strengths could be isolated experimentally in a near future.

However figure 13 provides a nice example of what a new approach of the data reduction and analysis methods can bring about. This figure shows the multipole strengths obtained from ^4He inelastic scattering experiments at two incident energies (340 and 480MeV) on three nuclei (^{58}Ni, ^{116}Sn, ^{208}Pb)/12/(see also these proceedings). In this work the data have been put in form of a two dimensionnal matrix $d^2\sigma/d\omega dE$, the background has been defined as a two dimensionnal surface using analytical functions, this procedure ensures automatically the continuity of the background angular distribution. After background subtraction, the bidimensionnal cross-section has been analysed by energy bins and fitted with combinations of DWBA calculated cross-section using a χ^2 procedure.

For the well known modes (GQR, GMR, isovector GDR) the results obtained are in agreement with those obtained from other works. In the higher continuum the multipole strengths displayed on figure 13 exhibit a few interesting features.

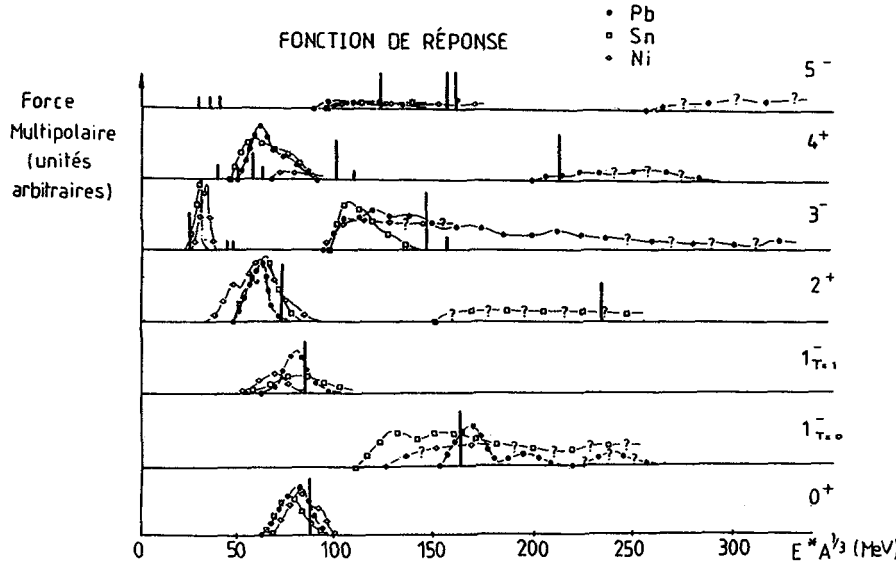

Fig. 13 : Multipole strength distributions obtained from ^4He scattering experiments in ^{208}Pb, ^{116}Sn and ^{58}Ni /12/.

Let us note first that these strengths show a rough $A^{-1/3}$ dependence. The isoscalar dipole strength in ^{208}Pb is found markedly higher ($E_x \sim 29$ MeV) here than in the experiments discussed in the preceding part of the talk. I have no explanation for the discrepancy. Some higher quadrupole strength is found in ^{116}Sn in the region where RPA calculations predict the first compressionnal quadrupole mode. It is also interesting to note the much more widespread octupole yield obtained here compared to other results /51/. Although the other strengths found are not affected with a very high degree of reliability and must be confirmed, the present result show that new methods of analysis can be developped which are more adjusted to the investigation of multipole strength widespread over the high lying nuclear continuum, and opens interesting prospects for the future of such studies.

REFERENCES

1 - Walecka J.D., Phys. Rev. 126 (1962) 653
2 - Marty N. et al., Orsay report IPNO 76-03
3 - Youngblood D.H. et al., Phys. Rev. Lett. 39 (1977) 1188
4 - Buenerd M., The giant monopole resonance in nuclei, Nuclear Physics, Dasso C.H., Broglia R.A., Winther A. (Eds), NHPC 1982
5 - Bohr A. and Mottelson B., Nuclear structure, Vol.II, Benjamin, 1975
6 - Auerbach N. and Yeverechyahu A., Ann. Phys. 95 (1975) 35
7 - Bertsch G., Nucl. Phys. A249 (1975) ; Les Houches Lectures 1977, session XXX, NHPC, Amsterdam, 1978
8 - Eckart G., Holzwarth G., and Da Providencia J.P., Nucl. Phys. A364 (1981) and refs. therein
9 - Hasse R.W., Glosh G., Winter J. and Lumbroso A., Phys. Rev. C 25 (1982 2771
10 - Wong C.Y. and Azziz N., Phys. Rev. C24 (1981) 2290
11 - de Haro R., Krewald S. and Speth S., Nucl. Phys. A388 (1982) 265
12 - Bonin B., thesis, Saclay report CEA-N-2337, 1983
13 - Decharge J. and Gogny D., private communication
14 - Blaizot J.P., Phys. Rep. 64 (1980) 171
15 - Jennings B.K. and Jackson A.D., Phys. Rep. 66 (1980) 141
16 - Youngblood D.H., in giant multipole resonances (F. Bertrand edit.) Harwood, N.Y. 1980
17 - Lebrun D., thesis, université de Grenoble, ISN report 81 - 37
18 - Morsch H.P. et al., Phys. Rev. C22 (1980) 489 ; Phys. Rev. C 25 (1982) 2939
19 - Bertrand F. et al., Phys. Rev. C 22 (1980) 1832
20 - Willis A. et al., Nucl. Phys. A344 (1980) 137
21 - Yamagata T. et al., Nucl. Phys. A381 (1982) 277
22 - Youngblood D.H. et al., Phys. Rev. C 23 (1981) 1997
23 - Buenerd M. et al., Phys. Lett. B 84 (1979) 305
24 - Satchler G.R., Particles and nuclei, 5 (1973) 195
25 - Buenerd M., and Lebrun D., Phys. Rev. C 24 (1981) 1356
26 - Morsch H.P., and Decowski P., Nucl. Phys. A377 (1981) 261 ; Izumoto T. et al., Phys. Rev. C24 (1981) 2179
27 - Lebrun D. et al., Phys. Lett. 97B (1980) 358
28 - Martin P. et al. Proc. RCNP int. symp. on highly excited states in nuclear reactions, ed. H. Ikegami and M. Muraola, Osaka university, 1980
29 - Brandenbury S. et al., communication to this conference ; Grobmayr P. et al., ibid. ; Willis A. et al., ibid.
30 - Buenerd M. et al., Phys. Rev. Lett. 45 (1980) 1667
31 - Garg U. et al., Phys. Rev. Lett. 45 (1980) 1670
32 - Abgrall Y. et al. Nucl. Phys. A346 (1980) 431 ; Arickx F. et al., Phys. Lett. 106B (1981) 275
33 - Faessler A. et al., Nucl. Phys. A230 (1974) 302 and ref. therein
34 - Beil H. et al., Nucl. Phys. A227 (1974) 427
35 - Werntz C. and Uberall H. Phys. Rev. 149 (1966) 762
36 - Kirson M. Nucl. Phys. A 257 (1976) 58
37 - Pandharipande V.R., Phys. Lett. 31B (1970) 635

38 - Krivine H., Treiner J. and Bohigas O., Nucl. Phys. A336 (1980) 155
39 - Hodgson P.E., 4th int. symp. on nucl. phys., Oaxtepec, Mexico, 1981
40 - Treiner J. et al., Nucl. Phys. A37 (1982) 253
41 - Buenerd M. et al., Lectures notes in Physics, Vol. 158, Springer Verlag, 1981 p.303
42 - Blaizot J.P. and Grammaticos B., Nucl. Phys. A355 (1981) 115
43 - Berman B.L., Gibson B.F. and O'connel J.S., Phys. Lett. 66B (1977) 405
44 - Van Giai N. and Sagawa H., Nucl. Phys. A371 (1981) 1
45 - Dumitrescu T.S. and Srr F.E., preprint NBI 82-5
46 - Morsch P. et al., phys. Rev. Lett. 45 (1980) 337 and preprint Julich, 1983
47 - Harakeh N. and Dieperink A.E.L., Phys. Rev. C23 (1981) 2329
48 - Djalali C. et al., Nucl. Phys. A380 (1982) 42
49 - Morsch P. et al., Phys. Lett. 119B (1982) 311
50 - Brack T., and Stocker W. Preprint
51 - See for example Speth J. and Van der Woude A., Rep. Prog. Phys. 44 (1981) 719
52 - Morris C.L., contribution to this conference.